Journal of Quantitative Spectroscopy & Radiative Transfer 133 (2014) 72–80

Contents lists available at ScienceDirect

Journal of Quantitative Spectroscopy & Radiative Transfer

journal homepage: www.elsevier.com/locate/jqsrt

Shaped beam scattering from a single lymphocyte cell by generalized Lorenz–Mie theory

Jia Jie Wang [a,*], Lu Han [a], Yi Ping Han [a], Gerard Gouesbet [b], Xuecheng Wu [c], Yingchun Wu [c]

[a] School of Science, Xidian University, Xi'an 710071, China
[b] Laboratoire d'Electromagnétisme des Systèmes Particulaires (LESP), UMR 6614 du CNRS, BP12, avenue de l'université, technôple du Madrillet, 76801 Saint-Etienne-du Rouvray, France
[c] State Key Laboratory of Clean Energy Utilization, Zhejiang University, Hangzhou 310027, China

ARTICLE INFO

Article history:
Received 20 May 2013
Received in revised form
10 July 2013
Accepted 12 July 2013
Available online 20 July 2013

Keywords:
Shaped beam scattering
Single nucleated cell
Eccentric stratified sphere
Lymphocyte cell
Gaussian beam
Generalized Lorenz–Mie theory

ABSTRACT

With the aim of improving the measurement capabilities of laser-based diagnostic instruments for cells, an eccentric stratified dielectric sphere model illuminated by an arbitrary shaped beam is applied to the modeling of light scattering by a single nucleated cell within the framework of the generalized Lorenz–Mie theory (GLMT). A particular attention is paid to the study of scattering properties of a lymphocyte cell from an arbitrary incident Gaussian beam. Numerical results concerning the influence of shaped beam parameters (beam waist radius, incident angle, location of beam center) as well as of cellular parameters (ratio of nucleus size to cell size, location of the nucleus within the cell) on the scattering properties are presented and discussed, with comparisons to the scattering behaviors from a concentric stratified sphere model. The results reveal that the forward scattering intensities are mainly determined by the cell size regardless of the nucleus/cell ratio, while sideward scattering signals are sensitive to the change of cell internal structure. As the beam waist radius varies, the scattering patterns in the present cases are similar to each other, although the absolute intensities are different. Additionally, location of the nucleus within the cell, incident angle of the beam as well as location of the beam waist center play significant effects on the light scattering intensity distributions.

© 2013 Elsevier Ltd. All rights reserved.

1. Introduction

The human white blood cells (WBCs), which are also known as leukocytes, are very important components in human blood due to their significant role in controlling various disease conditions and eliminating invading microorganisms. Five types of WBCs are normally found in human blood: two types of mononuclear (lymphocytes and monocytes) and three types of granulocytes (eosinophils, basophils, and neutrophils).

In normal conditions, lymphocytes occupy around 20–44% relative to all WBCs population. These cells play a highly important role in the human immunity against microorganisms and other sources of foreign macromolecules. Specifically, the T-lymphocytes constitute a large part of the human lymphocyte population, they act against virus infected cells and tumor cells, while the B-lymphocytes confer immunity through the production of specific, soluble antibodies. Their quantitative levels and morphological distribution are regarded as the most important indicators among others in clinical diagnosis and immunity research [1].

In recent years there has been an increasing interest in light scattering by lymphocytes due to the fact that light

* Corresponding author. Tel.: +86 02988200182.
E-mail address: wangjiajie@xidian.edu.cn (J.J. Wang).

0022-4073/$ - see front matter © 2013 Elsevier Ltd. All rights reserved.
http://dx.doi.org/10.1016/j.jqsrt.2013.07.012

scattering is able to provide an exquisitely sensitive approach for real-time, non-intrusive and sometimes label-free determination of cellular shape as well as internal structure, consequently leading to accurate cell identification and sorting. A prominent example of applications is the development of flow cytometry for cell discrimination based on light scattering signals [1–3].

With decades of improvement, advanced instruments, such as the scanning flow cytometry (SFC), are now able to perform the measurement of light scattering patterns of cells [2]. To obtain the cellular features based on the measured light scattering patterns, researchers normally turn to the comparison of experimental data with simulated results since there is no general solution for the inverse scattering problem. Thus, fulfilling the potential of light scattering techniques for cell diagnosis requires a continuous development of accurate as well as efficient characterization methods, the primary task being to develop a proper optical model for the scattering problem under study, and then to solve corresponding direct and inverse light scattering problems.

Concerning the optical model, the better we know the morphological features of cells and the description of the incident light, the more reliable solutions could be obtained and the more the problem of cell characterization is accurately solved. Generally, fundamental ingredients, including optical parameters and morphometric features, are needed to build a precise physical model for cells. On one hand, the optical parameters of cell constituent are still an open question since they are not available in a reliable, complete form, as we will discuss later in Section 3.1. On the other hand, the morphometric features of the cell are rather complex. It might take into consideration, for example, some nonsphericity of the cell and its nucleus, quantitative data on an eccentric nucleus location within the cell, cell surface texture, and so on.

Depending on the complexity of the cell structure, several optical models were proposed to the simulation of light scattering by cells along with the development of light scattering theories, including analytical methods, e.g. generalized Lorenz–Mie theory [4], various numerical methods, e.g. finite difference time domain method (FDTD) [5], discrete dipole approximation (DDA) [6], approximation methods, e.g. geometrical optics approximation (GOA) [7], and so on.

The simplest physical model available is the one of a homogeneous dielectric sphere. It was applied to the simulation of cell sizing by using the classical Lorenz–Mie Theory (LMT). It has been successfully used in the sizing of lymphocytes based on the light-scattering signals obtained from a flow cytometer by Neukammer et al. [8]. Nevertheless, this model is very sketchy and takes almost no account of cell morphology or internal structure. To extract more morphological characteristics of lymphocytes from experimental data, a more detailed model is required. The model of a two-layer concentric sphere is proposed by Aden and Kerker [9] and then extended to a multi-layer concentric sphere [10]. These models are much more adequate in the cell diagnosis since the inhomogeneity brought in by the nucleus is taken into consideration. Their advantages are proved in the analysis of nucleated blood cells, for instance, to discriminate abnormal mutated leukocytes caused by virus from normal healthy ones [11]. Also a five-layer model was shown to give a very good agreement between experimental and theoretical light-scattering profiles (LSPs) in the analysis of lymphocyte by Zharinov et al. [12].

Furthermore, through the observation of confocal microscopy, 3D images of a single lymphocyte can be obtained, and one slice of it is presented in the left part of Fig. 1. As we can see, lymphocytes are cells in a nearly spherical shape with clear, transparent cytoplasm and a large single spherical nucleus, which occupies more than 60% of the cell in volume. Additionally, the nucleus suspended within the cytoplasm is not always in the center of the cell. Based on these cellular features of lymphocytes, we could conclude that an eccentric stratified dielectric sphere model approaches to the cell in a greater extent than the concentric stratified sphere model. Nevertheless, due to the complexity of the eccentric sphere model, the calculation of corresponding light scattering problems is not a trivial task. Thus various numerical methods and approximation methods are applied in this study, e.g. finite difference time domain

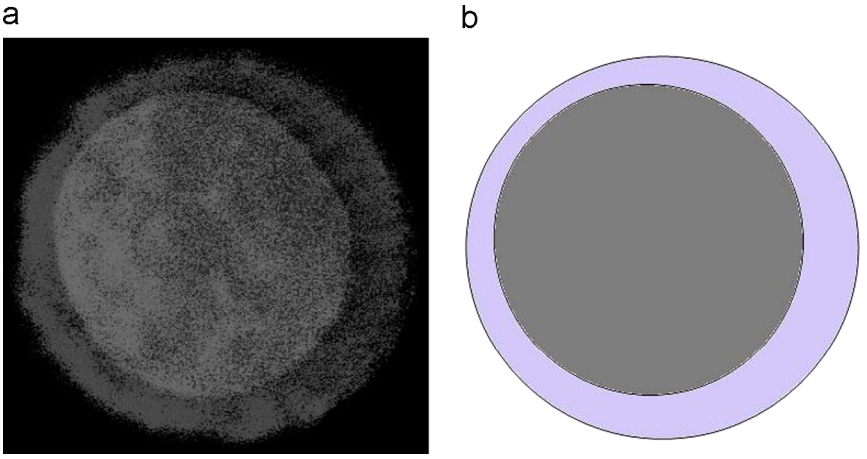

Fig. 1. (a) A slice from a confocal image of a lymphocyte and (b) optical model of a lymphocyte cell with an eccentric core.

method (FDTD) [5], discrete dipole approximation (DDA) [6], geometrical optics approximation (GOA) [7], and so on.

To find out to what extent realistic shape and structure of a cell affect its light scattering pattern, Brock et al. [5] constructed a 3D structure of lymphocytes from confocal images by using the FDTD. Hoekstra et al. [6] investigated the influence of the nucleus on the light scattering signals of lymphocytes by using a parallel fast DDA. Based on the geometrical–optics theory, the eccentric sphere model was applied to the modeling of single nucleated cell by Bu and Wang [7]. The Monte Carlo method was also applied to the simulation of leukocytes [13]. These results presented in the literature strongly show that eccentricity of the nucleus laid a significant influence on the scattering pattern when compared to those behaviors based on a single sphere model or a coated sphere, and that the scattering intensity is closely related to the location of the nucleus within the cell.

Although the various numerical methods mentioned above, such as FDTD, DDA, show their capabilities to give accurate results in the simulation of light scattering from cells, they are considered not effective enough in computations for the simulations of realistic cells in the resonance region, which makes them impractical in solving the inverse light scattering problems where angular scattering pattern has to be analyzed in real time. Compared to the numerical methods, analytical methods always provide an accurate but more effective way for the simulation of light scattering problems. Dating back to the well-known Lorenz–Mie theory, it provides a rigorous way to describe the electromagnetic scattering interaction between a linearly polarized plane wave and a homogeneous spherical particle. Since the advent of laser, the interaction of a focused laser beam with different kinds of particles has become a more interesting topic. To meet the requirements of these new practical cases, the LMT has been generalized after the name of generalized Lorenz–Mie theory mainly from two perspectives: (i) arbitrary laser beam and (ii) various particle shapes. With decades of efforts devoted to the development of GLMT, it now has been widely applied in various fields including particle sizing, Raman scattering diagnostics, optical manipulation, and design of new optics devices [14]. Recently, by using a successful description of an arbitrary oriented incident (oblique illumination) shaped beam in GLMT [15–19], the GLMT has been extended to the study of shaped beam scattering from a sphere with eccentrically located spherical inclusions. Scattered field in the far zone, internal as well as near field distribution have been analyzed [20,21]. In the present paper, the GLMT is applied to study the effect of inhomogeneity brought by the nucleus on the light scattering intensity distribution. As shown in the right part of Fig. 1, an eccentric stratified sphere model is built for a lymphocyte cell.

Additionally, most of the literature is concerned with the modeling of lymphocytes with an illumination of plane wave. However, in the modern laser-based scattering techniques, laser beams are focused to generate the scattering pattern of cells [22], or even tightly focused laser beams are applied to the trapping of cells [23]. For instance, in the apparatus of SFC, an array of particles passes through a tube sequentially one by one along a micro-fluid flow, which is illuminated by a laser beam. To generate a clear enough scattering pattern for the purpose of particle characterization, the probe laser beam is required to focus to cellular dimensions. In this case, the scattering of a particle in a sharply focused laser beam cannot be described by the conventional plane wave illumination based on the classical Lorenz–Mie theory, the influence of the laser beam parameters on the distribution of scattering intensity should be considered for a correct interpretation of the experimental data [22].

In the present study, a particular attention is paid to the analysis of shaped beam scattering from lymphocytes. Simulations of the scattering properties of lymphocytes under illumination by a shaped beam are carried out with the aim of developing an appropriate optical model to solve the light scattering problem for lymphocyte characterization. The body of the present paper is organized as follows. In Section 2, based on the optical model of lymphocyte, theoretical treatment for the scattering problem of an eccentric stratified sphere illuminated by an arbitrary shaped electromagnetic beam in an arbitrary incident direction is presented within the framework of GLMT. Particular attention is paid to the description of an arbitrary shaped beam for the scattering problem under study. In Section 3, the case of a focused Gaussian beam is specifically considered for numerical illustration. Intensity distributions of scattered fields are presented for various parameters of the incident laser beam and of the scattering system. Some discussions are presented in Section 4, which serves as a conclusion as well.

2. Theoretical treatment

2.1. Definition of the problem

The geometry of the specific scattering problem under study is illustrated in Fig. 2. The host sphere with a radius of R_c (c is short for cell) is attached to a global Cartesian coordinate system $O_1X_1Y_1Z_1$, and its corresponding spherical coordinates are designated as $(r_1, \theta_1, \varphi_1)$. A spherical inclusion with a radius of R_n (n is short for nucleus) is embedded in the host sphere. It is attached to an inclusion coordinate system $O_2X_2Y_2Z_2$, whose corresponding spherical coordinates are designated as $(r_2, \theta_2, \varphi_2)$. The three axes in the inclusion coordinate system are parallel to the corresponding axes in the global coordinate system, correspondingly.

Without any loss of generality, the center of the inclusion is located on the z axis of the global coordinate system. The displacement of inclusion center is designated by d, we have

$$x_2 = x_1, \quad y_2 = y_1, \quad z_2 = z_1 - d \tag{1}$$

The refractive index and wave number of the surrounding medium are m_s and k_s, respectively. The corresponding parameters for the host sphere are m_c and k_c, and for the inclusion are m_n and k_n. The ratio of nucleus size to cell diameter is defined as R_n/R_c, and the eccentric-rate of nucleus within the cell is given as d/R_c.

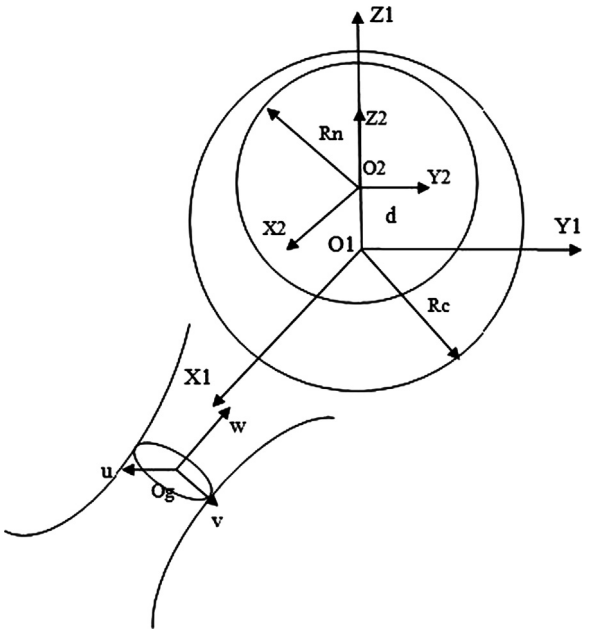

Fig. 2. Illustration of shaped beam scattering problem under study.

The scattering model in Fig. 2 is illuminated by an arbitrary shaped beam propagating along the w axis in the beam coordinate system O_guvw. The coordinates of its origin O_g with respect to the global coordinate system $O_1X_1Y_1Z_1$ are denoted as (x_0, y_0, z_0). The system $O_1X_1Y_1Z_1$ can be obtained from the beam coordinate system O_guvw by rotations through Euler angles (α, β, γ) followed by a translation of (x_0, y_0, z_0), and vice versa. Specifically, in this paper, a focused Gaussian beam propagating along the w axis with beam waist center located in the origin of the beam coordinate system O_guvw is applied for numerical computations. Its electric component is linearly polarized in the v-direction at the waist. The time-dependence factor reading as $\exp(i\omega t)$ is assumed, where ω is the angular frequency.

2.2. Generalized Lorenz–Mie theory

The theoretical treatment of scattering from an eccentric stratified sphere illuminated by an arbitrary shaped beam was originally presented by Gouesbet and Gréhan [24]. Afterward, Han et al. [25] and Yan et al. [26] numerically studied this problem for the case of on-axis illumination. Recently, with a successful description of an arbitrary shaped beam with an arbitrary incident angle (oblique illumination) within the framework of GLMT [15–19], a sphere with an eccentrically located spherical inclusion scattered from an arbitrary incident laser beam was studied, and numerical results concerning scattered field in the far zone [20], internal and near field distribution [21] were presented. Here, we will not focus on these derivations but recall some expressions necessary for the sequel.

In the global coordinate system, an arbitrary shaped beam in an arbitrary orientation illuminating the host sphere may be expressed in terms of spherical vector wave functions (VSWFs) with two sets of expansion coefficients (a_{mn}, b_{mn}):

$$\mathbf{E}^{inc} = E_0 \sum_{n=1}^{\infty} \sum_{m=-n}^{n} a_{nm}\mathbf{M}_{nm}^{(1)}(k_s\mathbf{r}_1) + b_{nm}\mathbf{N}_{nm}^{(1)}(k_s\mathbf{r}_1) \tag{2}$$

in which the field strength E_0 will be numerically taken equal to unity.

The relationship between the expansion coefficients (a_{mn}, b_{mn}) on one hand and the more traditional beam shape coefficients ($g_{n,TM}^{m}$, $g_{n,TE}^{m}$)on the other hand is available from [27] and will be provided in the sequel Section 2.3.

The scattered field outside of the host sphere and the field in the annular zone between the surface of the host sphere and that of the inclusion may similarly be expressed in the global coordinate system with two sets of expansion coefficients:

$$\mathbf{E}^{sca} = E_0 \sum_{n=1}^{\infty} \sum_{m=-n}^{n} c_{nm}\mathbf{M}_{nm}^{(4)}(k_s\mathbf{r}_1) + d_{mn}\mathbf{N}_{nm}^{(4)}(k_s\mathbf{r}_1) \tag{3}$$

$$\mathbf{E}^{int1} = E_0 \sum_{n=1}^{\infty} \sum_{m=-n}^{n} e_{nm}\mathbf{M}_{nm}^{(3)}(k_c\mathbf{r}_1) + f_{mn}\mathbf{N}_{nm}^{(3)}(k_c\mathbf{r}_1) + v_{nm}\mathbf{M}_{nm}^{(4)}(k_c\mathbf{r}_1) + h_{mn}\mathbf{N}_{nm}^{(4)}(k_c\mathbf{r}_1) \tag{4}$$

The same operations are then carried out in the inclusion coordinate system, in which the field in the annular zone and the internal field inside of the inclusion might be represented as

$$\mathbf{E}^{int1} = E_0 \sum_{n=1}^{\infty} \sum_{m=-n}^{n} r_{nm}\mathbf{M}_{nm}^{(3)}(k_c\mathbf{r}_2) + s_{mn}\mathbf{N}_{nm}^{(3)}(k_c\mathbf{r}_2) + t_{nm}\mathbf{M}_{nm}^{(4)}(k_c\mathbf{r}_2) + u_{mn}\mathbf{N}_{nm}^{(4)}(k_c\mathbf{r}_2) \tag{5}$$

$$\mathbf{E}^{int2} = E_0 \sum_{n=1}^{\infty} \sum_{m=-n}^{n} p_{nm}\mathbf{M}_{nm}^{(1)}(k_n\mathbf{r}_2) + q_{mn}\mathbf{N}_{nm}^{(1)}(k_n\mathbf{r}_2) \tag{6}$$

To solve the scattering problem, three steps are carried out. Firstly, in the global coordinate system, the expansion coefficients that describe the scattered field, (c_{mn}, d_{mn}), and the expansion coefficients that describe the main field (e_{mn}, f_{mn}, v_{mn}, h_{mn}), are related to the expansion coefficients that describe the incident field (a_{mn}, b_{mn}) by application of the boundary conditions in the host sphere surface, according to which the tangential components of the electric and magnetic fields are continuous across the surface. Then similarly, in the inclusion coordinate system, the expansion coefficients which describe the inclusion internal field (p_{mn}, q_{mn}), are related to the expansion coefficients describing the main field (r_{mn}, s_{mn}, t_{mn}, u_{mn}), by application of the corresponding boundary conditions at the surface of the inclusion. Finally, the solutions to the scattering problem can be readily reached by applying translational addition theorems of VSWFs to the field in the annular zone. For details which are not provided here, the reader is kindly requested to refer to Ref. [24].

2.3. Description of shaped beam

In the GLMT, the electromagnetic components of the illuminating beam are described by multiple expansions over a set of basic functions, and the expansion coefficients are usually denoted as $g_{n,X}^{m}$ (X is TE, transverse electric, or

TM, transverse magnetic, with n from 1 to ∞, m from $-n$ to n), are known as beam shape coefficients (BSCs). These BSCs are used to express electromagnetic fields of laser beams in expanded forms, for use in GLMTs, or in other light scattering approaches such as in the Extended Boundary Condition Method (EBCM). Their calculations form the key issue as well as the most difficult one, when dealing with a GLMT.

In the particle coordinate system, the relationships between the expansion coefficients (a_{mn}, b_{mn}) on one hand, and the BSCs ($\widetilde{g^m_{n,TM}}$, $\widetilde{g^m_{n,TE}}$) on the other hand read as [16,20,27]

$$b_{mn} = kc_n^{pw}(-1)^{(m-|m|)/2}\frac{(n-m)!}{(n-|m|)!}\widetilde{g^m_{n,TM}}$$
$$a_{mn} = -ikc_n^{pw}(-1)^{(m-|m|)/2}\frac{(n-m)!}{(n-|m|)!}\widetilde{g^m_{n,TE}} \quad (7)$$

in which c_n^{pw} are coefficients which naturally appear in the Bromwich formulation of the LMT. While the BSCs in the particle coordinate system ($\widetilde{g^m_{n,TM}}$, $\widetilde{g^m_{n,TE}}$) are related with the BSCs in the beam coordinate system ($g^m_{n,TM}$, $g^m_{n,TE}$) as

$$\widetilde{g^m_{n,X}} = \mu_{mn}\sum_{s=-n}^{n}\frac{H^m_{sn}(\alpha,\beta,\gamma)}{\mu_{sn}}g^s_{n,X} \quad (8)$$

$$\mu_{mn} = (-1)^{(m-|m|)/2}\frac{(n-|m|)!}{(n-m)!} \quad (9)$$

$$H^m_{sn}(\alpha,\beta,\gamma) = \sqrt{\frac{(n-m)!(n+s)!}{(n+m)!(n-s)!}}e^{is\alpha}(-1)^{m+s}d^{(n)}_{sm}(\beta)e^{im\gamma} \quad (10)$$

in which (α,β,γ) are Euler angles bringing the beam coordinate system to the scatterer coordinate system, whose definitions could be found in any of the references [15–19].

With decades of efforts devoted to the description of an arbitrary shaped beam, the BSCs of an arbitrary shaped beam in the beam coordinate system can be evaluated by several methods, sharing various degrees of time running efficiency, or of flexibility, namely by using quadratures [28], finite series [29], localized approximations generating localized beam models [30,31], or by a hybrid method taking advantage of both quadratures and of a localized approximation, named the integral localized approximation [32]. The evaluation of BSCs has also been investigated by relying on addition theorems for translations of coordinate systems, an approach originally introduced by Doicu and Wriedt [33] and also used by Zhang and Han [34].

In our computer program, the modified localized approximation method, which was rigorously justified by Gouesbet and Lock [35,36], is applied to evaluate the BSCs in the unrotated coordinate system due to the fact that it provides the most efficient method, with regard to computational times, by orders of magnitude with respect to other methods, such as by using quadratures. It is also the most appealing from a physical point of view because it provides many physical insights on the interpretation of beam models.

3. Numerical results

To validate the presented theoretical treatment and computation codes, simulated results for angular scattering distributions as well as for field intensity distributions are obtained for cases similar to those given in the literature. Examples for these computation cases are made for either a homogeneous sphere or a coated sphere illuminated with a plane wave or a shaped beam, and have been compared with previously published data in the literature [37,38]. Some of the comparisons and discussions were shown in our previous papers [21,22]. No differences were noticed in the studied cases. In the following we will analyze the scattering properties of lymphocytes by using the method presented above.

3.1. Parameters of lymphocyte

As noted above, besides morphometric components, optical parameters are also needed to build a complete lymphocyte model. So far, the size parameters, the refractive index distributions in cell constituents are not always available at least in reliable and complete form due to the complexity of the lymphocytes. In the present simulations, to study the effect of inhomogeneity brought by an eccentric nucleus and the influence of shaped beam illumination on light scattering pattern, the optical parameters of the lymphocytes published in literature are used.

According to a review by Strokotov et al. [39], the mean diameter of lymphocyte reported in the literatures ranges from 6.7 μm to 7.3 μm for normal donors as determined by the Coulter principle, the results were 5.4–6.5 μm by electron microscopy and a range from 6.4 μm to 8.3 μm was obtained by using optical microscopy. As we can see, the mean diameter of lymphocyte ranges from 6.0 to 8.3 μm for the cell size due to different approaches, but shows no significant differences. In the present simulations, a mean value of cell diameter is assumed to be 6.4 μm based on the measurement by electron microscopy [39].

The mean value of the cytoplasmic refractive index of human lymphocytes in peripheral blood may be reliably taken as $m_c = 1.3765$, but it is worth to mention that this is an effective refractive index of the whole cytoplasm, including all granules and other inclusions, while the value for the ground substance of the cytoplasm is a bit lower. The average refractive index of nucleus is assumed $m_n = 1.4476$.

In contrast to the small uncertainty in the mean value of lymphocyte size, the mean ratio of nucleus size to cell diameter R_n/R_c varies much more. The ratio determined by electron microscopy ranges from 0.56 to 0.7844 [40], and it varied from 0.82 to 0.90 for three healthy donors as determined by optical microscopy [41]. Thus, a ratio of nucleus to cell diameter in the range of $R_n/R_c = 0.60$–0.90 is taken in this study to investigate its influence on the scattering pattern.

In a summary, the following cellular characteristics are used in the present simulations for the scattering from a single lymphocyte: cell diameter Dc=6.4 μm, ratio of nucleus and cell diameters R_n/R_c in the range of [0.6, 0.9], refractive index of cytoplasm $m_c = 1.3765$ and that of nucleus $m_n = 1.4476$. The refractive index of the surrounding medium is assumed to be 1.337.

Furthermore, since the main purpose of the present paper is to carry out a theoretical study of lymphocyte cells' scattering properties, which will focus on the analysis of angular distributions of scattering intensity instead of on the

scattering effects (optical force or torque exerted on the cell), a Gaussian beam with a wavelength of 632.8 nm is applied assuming that the incident laser was provided by a He–Ne laser. This dates back to the fact that Gaussian beams with wavelengths within the range of visible light could be applied as probe beams in an optical tweezers to observe the real-time motions of particles, and they could also be used as probe beams in the laser-based SFC instruments. Nevertheless, it is worth to notice that in practical experiments, laser beams with a relatively small power is suggested since a living cell might be hurt through heating.

3.2. Influence of ratio of nucleus size to cell size

Firstly, the influence of ratio of nucleus size to cell diameters R_n/R_c on the light scattering pattern is studied. Fig. 3 shows the angular distributions of scattering intensities for a concentric sphere and an eccentric sphere ($d=0.1R_c$ along the positive z axis), which is illuminated by a plane wave propagating along the positive z axis. A range of $R_n/R_c=0.60$–0.90 is considered.

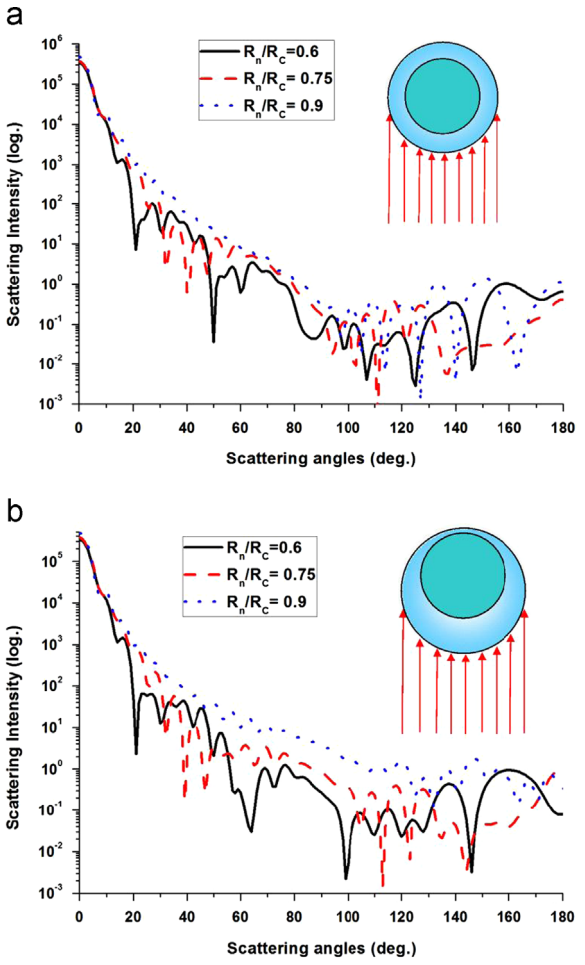

Fig. 3. Angular distributions of scattering intensity for lymphocytes with various nucleus/cell size ratios in a case of plane wave illumination. (a) Concentric sphere and (b) eccentric sphere with $d=0.1R_c$.

As we can see, the intensity behaviors for cells with different nucleus/cell size ratios in the forward direction (less than 10°) are almost the same. And, in general, the scattering distribution of a lymphocyte with larger nucleus is much smoother than that with a smaller nucleus, for instance, in the sideward directions (20–50°). This might be due to the enhanced interference between the scattering of nucleus and that of the cell. The results obtained here agree with the previous results that forward scattering (FS) signals were considered to be proportional to the cell size, whereas side scattering (SS) signals have been shown to provide more information on the internal structure of the cells.

3.3. Influence of beam waist radius

To investigate the effects arising from the change of beam waist radius, angular distributions of scattering intensities for various beam shape radii are displayed in Fig. 4 for an eccentric sphere ($d=0.2R_c$ along the positive z axis) in cases of on-axis illumination as well as in cases of off-axis illumination. The ratio of nucleus size to cell

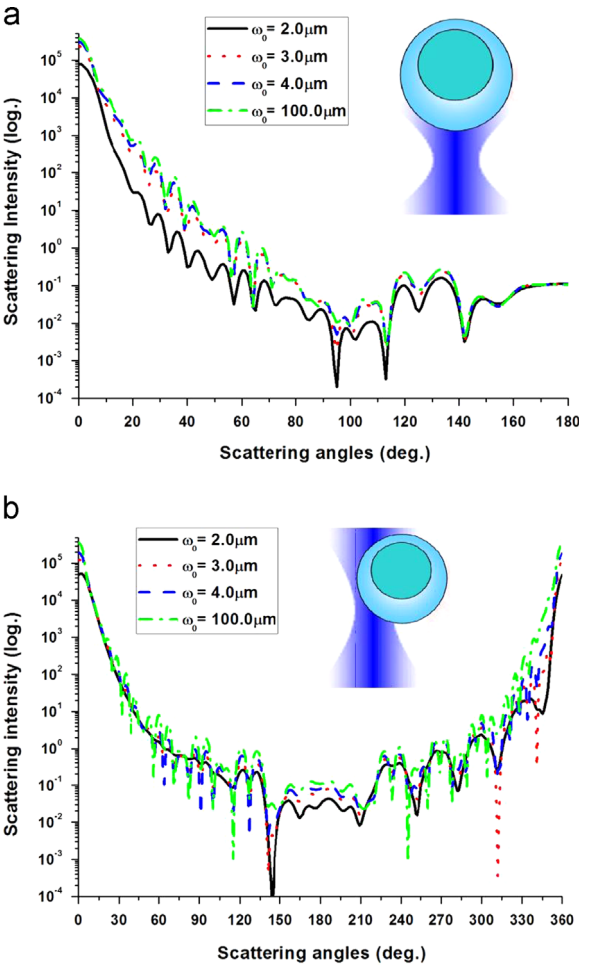

Fig. 4. Angular distributions of scattering intensity for an eccentric sphere ($d=0.2R_c$ along+z axis) illuminated by a Gaussian beam with various beam waist radius $R_n/R_c=0.75$. (a) On-axis Gaussian beam illumination and (b) off-axis Gaussian beam illumination.

diameter is 0.75. The location of the beam waist center in the case of off-axis illumination is $(0.25R_n, 0.0, 0.0)$. A scattering profile from 0° to 360° is plotted due to the breakdown of symmetry in the case of off-axis illumination.

It reveals that both for an on-axis illumination and for an off-axis illumination of the Gaussian beam, the scattering intensity pattern decreases as a whole as the beam waist radius decreases. This is due to the fact that, in our calculations, the largest intensity of the incident laser beam, which is located at the beam waist center, is assumed to be unit, whatever the other beam parameters.

Furthermore, it is interesting to observe that the scattering patterns for different beam waist radii are similar to each other, although the similarities in the cases of off-axis illumination are less visible.

3.4. Influence of location of beam waist center

In practical measurements, the symmetry of the scattering problem is hard to keep even for symmetric scatterer due to the shift of focused shaped laser beam. Therefore, the angular distributions of scattering intensities are displayed in

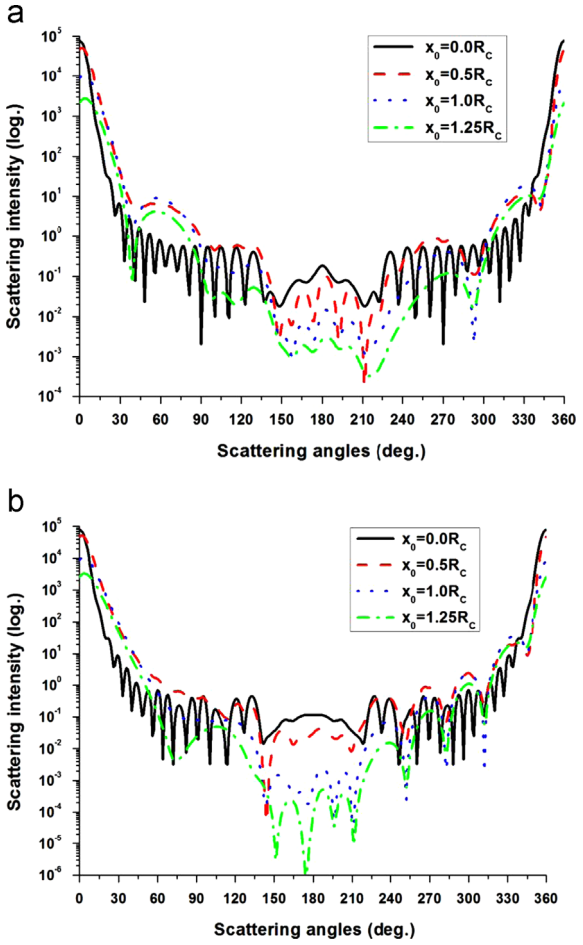

Fig. 5. Angular distributions of scattering intensity for (a) a concentric sphere (b) an eccentric sphere (R_n/R_c=0.75, $d=0.2R_c$ along the positive z axis), in a case of Gaussian beam illumination with different shifts of beam location.

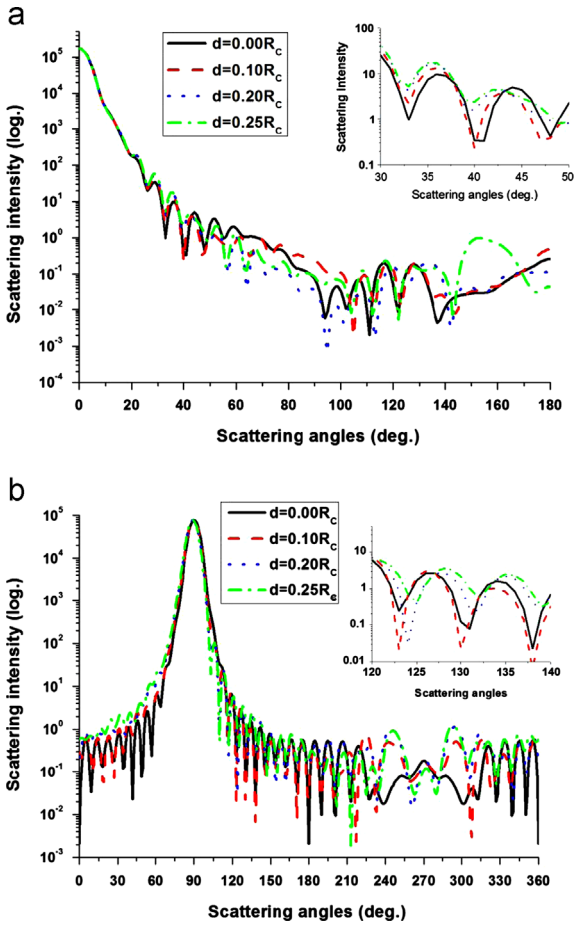

Fig. 6. Angular distributions of scattering intensity for lymphocytes with (a) nucleus translated along the beam propagation direction, (b) nucleus translated perpendicular to the beam propagation direction; in cases of on-axis Gaussian beam illumination ω_0=2.0 μm, R_n/R_c=0.75.

Fig. 5 for a concentric sphere and for an eccentric sphere (R_n/R_c=0.75, $d=0.2R_c$ along the positive z axis), in cases of Gaussian beam illumination with different shifts of beam location. The beam waist radius is 2.0 μm. The location of the beam center is shifted from the origin ($x_0=0.0$) of the cell to the edge of the cell ($x_0=1.25R_c$).

It is obvious to notice that as the beam waist center shifts away from the origin of the cell, the intensity drops dramatically in the backward scattering direction, and high oscillations on the scattering profile smooth out.

3.5. Influence of location of nucleus within the cell

As reported by Strokotov et al. [8], when nucleus is relatively large ($R_n/R_c=0.9$), the shift of nucleus shows no considerable effect on the structure of the light scattering profile, except for scattering angles larger than 40°.

To check the validation of this result for smaller ratios of nucleus size to cell size, angular distributions of scattered field are displayed in Fig. 6 for various positions of the nucleus, including cases when the nucleus shifts along the propagation direction of laser beam and when it shifts perpendicularly to the propagation direction of laser beam.

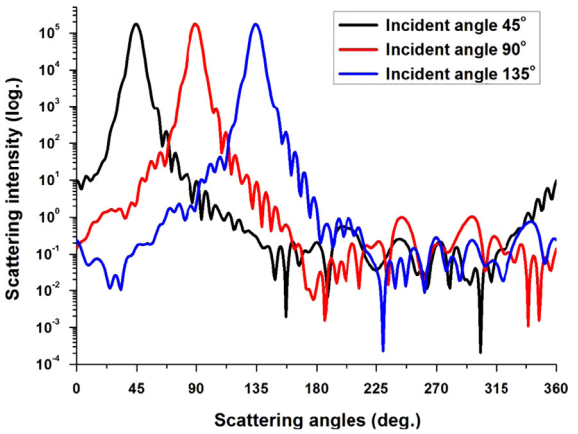

Fig. 7. Angular distributions of scattering intensity for an eccentric sphere ($R_n/R_c=0.75$, $d=0.2R_c$) in cases of on-axis Gaussian beam illumination with various incident angles.

The ratio of nucleus size to cell size is assumed to be $R_n/R_c=0.75$. The numerical results show that the location of the nucleus within the cell plays a significant effect on the light scattering intensity distribution.

A close inspection of Fig. 6(a) reveals that as long as the nucleus is situated along the propagation direction of the incident beam, e.g. the center of the nucleus is shifted from the front of the cell ($d=0.25R_c$) to the back of the cell ($d=-0.25R_c$), the intensity is prominent in the forward direction (0–20°) with an dramatic decay. The intensity becomes much more oscillating for larger scattering angles. It is interesting to notice that, for the scattering angle around 35°, a correlation between the scattering intensity and the location of nucleus might be able to be found due to the fact that the more the nucleus shift backwards, the lower the scattering intensity is [6]. Nevertheless, this correlation is not true for the cases of nucleus shifts perpendicularly to the beam propagation direction, as we could see from Fig. 6(b). Additionally, a whole picture of scattering profile is plotted in Fig. 6(b) since the symmetry of the scattering pattern is broken for the cases of nucleus shifts perpendicularly to the beam propagation direction.

3.6. Influence of incident angle

Due to the breaking of the scattering symmetry, the influence of incident angle of laser beam is studied with a change of incident angle from 0° to 180° with a step of 15°. Typical results are shown in Fig. 7.

As expected, the symmetry of the scattering intensity profile is broken down with a different decay rate in the forward-like directions, e.g. the intensity decreases faster on one side while slower on the other side.

4. Conclusion

A precise modeling of light scattering by biological cells requires not only the theoretical method of high accuracy but also proper cellular parameters and beam parameters as fundamental input information to ensure an accurate optical model. With the aim of improving laser-based optical techniques for cell characterization (for instance, the SFC for the analysis of leukocytes in human peripheral blood), an eccentric stratified dielectric sphere model illuminated by an arbitrary shaped beam is applied to the modeling of laser scattering by a single lymphocyte. Nevertheless, it is worth mentioning that the optical model of shaped beam scattering from an eccentric sphere within the framework of GLMT could also be applied to the simulations of other biological cell with a single nucleus.

In the present paper, particular attention is paid to the study of scattering properties of a lymphocyte from an arbitrary incident Gaussian beam. Numerical results concerning the influence of various parameters of cell and of Gaussian beam, including beam waist radius, location of the beam center, ratio of nucleus size to cell diameter, location of nucleus within the cell, and so on, on the scattering properties are presented and discussed. It can be demonstrated from these simulations that the forward scattering intensities are mainly determined by the gross cell size regardless of the nucleus/cytoplasm ratio while sideward scattering signals are sensitive to the changes of cell internal structure. As the beam waist radius varies, the scattering patterns in the present cases are similar to each other, although the absolute intensities are different. With a different incident angle of shaped laser beam, the symmetry of the scattering pattern is broken with a different dramatic decay in the forward direction. Furthermore, location of the nucleus within the cell as well as location of the beam waist center also plays significant effects on the light scattering intensity distribution.

Compared to the optical model of symmetric particles (homogeneous sphere, concentric layered sphere) illuminated by a plane wave applied in most of the literature, the eccentric stratified sphere model illuminated by a shaped beam, which represents more detailed structural features of the lymphocytes and of the incident beam, will lead to more accurate simulation data. Furthermore, due to the fact that the morphology of cell is rather complex, i.e. sometimes it shows a spheroidal shape, further studies will be required to analyze the influence of variations in shape, both for the cell and the nucleus, on the light scattering pattern.

Acknowledgment

The authors gratefully acknowledge the support by the “Fundamental Research Funds for the Central University” in China and “The Open Fund of State Key Laboratory of Clean Energy Utilization in Zhejiang University”. The authors thank the reviewers for providing several constructive comments and suggestions to the present paper.

References

[1] Constantinescu SP, Gancevich G. Electron optic possible resolution of basic proteins in the eosinophil leucocyte granules. Arch Roum Pathol Exp Microbiol 1972;31:455–8.
[2] Strokotov DI, Moskalensky AE, Nekrasov VM, Maltsev VP. Polarized light-scattering profile-advanced characterization of nonspherical

particles with scanning flow cytometry. Cytometry Part A 2011;79A:570–9.
[3] Maltsev VP, Hoekstra AG, Yurkin MA. Optics of white blood cells: optical models, simulations, and experiments. Exp Tech 2011;4:3.
[4] Lock JA, Gouesbet G. Generalized Lorenz–Mie theory and applications. J Quant Spectrosc Radiat Transfer 2009;110:800–7.
[5] Brock RS, Hu XH, Weidner DA, Mourant JR, Lu JQ. Effect of detailed cell structure on light scattering distribution: FDTD study of a B-cell with 3D structure constructed from confocal images. J Quant Spectrosc Radiat Transfer 2006;102:25–36.
[6] Hoekstra AG, Grimminck MD, Sloot PMA. Large scale simulations of elastic light scattering by a fast discrete dipole approximation. Int J Mod Phys C 1998;9:87–102.
[7] Bu M, Wang YW. Scattering analysis for eccentric-sphere model of single-nuclear cell. Proceedings of the 2011 Symposium on Photonics and Optoelectronics (SOPO).IEEE; 1–4.
[8] Neukammer J, Gohlke C, Höpe A, Wessel T, Rinneberg H. Angular distribution of light scattered by single biological cells and oriented particle agglomerates. Appl Opt 2003;42:6388–97.
[9] Aden AL, Kerker M. Scattering of electromagnetic waves from two concentric spheres. J Appl Phys 1951;22:1242–6.
[10] Wu Z, Wang Y. Electromagnetic scattering for multilayered sphere: recursive algorithms. Radio Sci 1991;26:1393–401.
[11] Ruban GI, Berdnik VV, Marinitch DV, Goncharova NV, Loiko VA. Light scattering and morphology of the lymphocyte as applied to flow cytometry for distinguishing healthy and infected individuals. J Biomed Opt 2010;15:057008–9.
[12] Zharinov A, Tarasov P, Shvalov A, Semyanov K, Van Bockstaele DR, Maltsev V. A study of light scattering of mononuclear blood cells with scanning flow cytometry. J Quant Spectrosc Radiat Transfer 2006;102:121–8.
[13] Cui J, Acton ST, Lin ZA. Monte Carlo approach to rolling leukocyte tracking in vivo. Med Image Anal 2006;10:598.
[14] Gouesbet G, Gréhan G. Generalized Lorenz–Mie Theories. Springer; 2011.
[15] Gouesbet G, Wang JJ, Han YP. Transformations of spherical beam shape coefficients in generalized Lorenz–Mie theories through rotations of coordinate systems: I. General formulation. Opt Commun 2010;283:3218–25.
[16] Wang JJ, Gouesbet G, Han YP. Transformations of spherical beam shape coefficients in generalized Lorenz–Mie theories through rotations of coordinate systems: II. Axisymmetric beams. Opt Commun 2010;283:3226–34.
[17] Gouesbet G, Wang JJ, Han YP. Transformations of spherical beam shape coefficients in generalized Lorenz–Mie theories through rotations of coordinate systems: III. Special values of Euler angles. Opt Commun 2010;283:3235–43.
[18] Gouesbet G, Wang JJ, Han YP, Gréhan G. Transformations of spherical beam shape coefficients in generalized Lorenz–Mie theories through rotations of coordinate systems. IV. Plane waves. Opt Commun 2010;283:3244–54.
[19] Gouesbet G, Lock JA, Wang JJ, Gréhan G. Transformations of spherical beam shape coefficients in generalized Lorenz–Mie theories through rotations of coordinate systems. V. Localized beam models. Opt Commun 2011;284:411–7.
[20] Wang JJ, Gouesbet G, Gréhan G, Han Y, Saengkaew S. Morphology-dependent resonances in an eccentrically layered sphere illuminated by a tightly focused off-axis Gaussian beam: parallel and perpendicular beam incidence. J Opt Soc Am A 2011;28:1849–59.
[21] Wang JJ, Gouesbet G, Han Y, Gréhan G. Study of scattering from a sphere with an eccentrically located spherical inclusion by generalized Lorenz–Mie theory: internal and external field distribution. J Opt Soc Am A 2011;28:24–39.
[22] Sloot P, Hoekstra AG, van der Liet H, Figdor CG. Scattering matrix elements of biological particles measured in a flow through system: theory and practice. Appl Opt 1989;28:1752–62.
[23] Doornbos RM, Schaeffer M, Hoekstra AG, Sloot P, Grooth BGd, Greve J. Elastic light-scattering measurements of single biological cells in an optical trap. Appl Opt 1996;35:729–34.
[24] Gouesbet G, Gréhan G. Generalized Lorenz–Mie theory for a sphere with an eccentrically located spherical inclusion. J Mod Opt 2000;47:821–37.
[25] Han G, Han Y, Liu J, Zhang Y. Scattering of an eccentric sphere arbitrarily located in a shaped beam. J Opt Soc Am B 2008;25:2064–72.
[26] Yan B, Han Xe, Ren KF. Scattering of a shaped beam by a spherical particle with an eccentric spherical inclusion. J Opt A: Pure Appl Opt 2009;11:015705.
[27] Gouesbet G. T-matrix formulation and generalized Lorenz–Mie theories in spherical coordinates. Opt Commun 2010;283:517–21.
[28] Gouesbet G, Letellier C, Ren K, Gréhan G. Discussion of two quadrature methods of evaluating beam-shape coefficients in generalized Lorenz–Mie theory. Appl Opt 1996;35:1537–42.
[29] Gouesbet G, Gréhan G, Maheu B. Expressions to compute the coefficients gmn in the generalized Lorenz–Mie theory using finite series. J Opt 1988;19:35.
[30] Gouesbet G. Validity of the localized approximation for arbitrary shaped beams in the generalized Lorenz–Mie theory for spheres. J Opt Soc Am A 1999;16:1641–50.
[31] Gouesbet G, Lock JA, Gréhan G. Generalized Lorenz–Mie theories and description of electromagnetic arbitrary shaped beams: localized approximations and localized beam models. J Quant Spectrosc Radiat Transfer 2011;112:1–27.
[32] Ren KF, Gouesbet G, Gréhan G. Integral localized approximation in generalized Lorenz–Mie theory. Appl Opt 1998;37:4218–25.
[33] Doicu A, Wriedt T. Computation of the beam-shape coefficients in the generalized Lorenz–Mie theory by using the translational addition theorem for spherical vector wave functions. Appl Opt 1997;36:2971–8.
[34] Zhang H, Han Y. Addition theorem for the spherical vector wave functions and its application to the beam shape coefficients. J Opt Soc Am B 2008;25:255–60.
[35] Lock JA, Gouesbet G. Rigorous justification of the localized approximation to the beam-shape coefficients in generalized Lorenz–Mie theory. I. On-axis beams. J Opt Soc Am A 1994;11:2503–15.
[36] Gouesbet G, Lock JA. Rigorous justification of the localized approximation to the beam-shape coefficients in generalized Lorenz–Mie theory. II. Off-axis beams. J Opt Soc Am A 1994;11:2516–25.
[37] Khaled EE, Hill SC, Barber PW. Light scattering by a coated sphere illuminated with a Gaussian beam. Appl Opt 1994;33:3308–14.
[38] Ngo D, Videen G, Chýlek PA. FORTRAN code for the scattering of EM waves by a sphere with a nonconcentric spherical inclusion. Comput Phys Commun 1996;99:94–112.
[39] Strokotov DI, Yurkin MA, Gilev KV, Van Bockstaele DR, Hoekstra AG, Rubtsov NB, et al. Is there a difference between T-and B-lymphocyte morphology? J Biomed Opt 2009;14:064012–36.
[40] Ruban GI, Kosmacheva SM, Goncharova NV, Van Bockstaele D, Loiko VA. Investigation of morphometric parameters for granulocytes and lymphocytes as applied to a solution of direct and inverse light-scattering problems. J Biomed Opt 2007;12:044011–7.
[41] Loiko VA, Ruban GI, Gritsai OA, Gruzdev AD, Kosmacheva SM, Goncharova NV, et al. Morphometric model of lymphocyte as applied to scanning flow cytometry. J Quant Spectrosc Radiat Transfer 2006;102:73–84.